

Identification of the key parameters in a mathematical model of PAR1-mediated signaling in endothelial cells

Leonardo Lenoci¹, Heidi E. Hamm¹, Emmanuele DiBenedetto^{2,*}

1 Department of Pharmacology, Vanderbilt University, Nashville, Medical Center, TN 37232, USA

2 Department of Mathematics, Vanderbilt University, Nashville, TN 37240, USA

* E-mail: em.diben@vanderbilt.edu

Abstract

Biophysical models are often populated by a large number of input parameters that are difficult to predict or measure experimentally. The validity and robustness of a given model can be evaluated by a sensitivity test to its input parameters. In this study, we performed local (based on a Taylor-like method) and global sensitivity (based on Monte Carlo filtering techniques) analyses of a previously derived PAR1-mediated activation model of endothelial cells. This activation model previously demonstrated that peptide-activated PAR1 has a different receptor/G-protein binding affinity that favors $G\alpha_q$ activation over $G\alpha_{12/13}$ by approximately 800-fold. Interestingly, the present study shows that the parameter regulating the binding rate of activated PAR1 to $G\alpha_{12/13}$ is indeed important to obtain the expected RhoGTP response. Moreover, we show that the parameters representing the rate of PAR1 deactivation and the rate of PAR1 binding to G_q , are the most important parameters in the system. Finally, we illustrate that the kinetic model considered in this study is robust and we provide complementary insights into the biological meaning and importance of its kinetic parameters.

Introduction

Mathematical models of biophysical phenomena often involve a large number of input parameters [1–5], such as reaction rates and initial concentrations, that must be either measured experimentally or inferred from similar biological systems. Moreover, experimentally measured parameters carry uncertainties due to experimental limitations, statistical analysis and different experimental conditions. One of the major goals in systems biology is to estimate how sensitive a computational model is to variations of its parameters

and study the effect of the parameter uncertainties on the model response. Sensitivity analysis aims at determining which parameters have the most influence on a predicted system behavior [6–9]. When the notion of “influence” is made quantitatively precise, sensitivity analysis can constitute a reliable robustness test for computational models [10].

In this study, we performed sensitivity analysis on the mathematical model of PAR1-mediated activation of endothelial cells of [4]. A schematic representation of the main signaling pathways analyzed in [4] is shown in Fig. 1. A specific PAR1 agonist, SFLLRN, simultaneously activates two classes of G proteins: G_q and $G_{12/13}$ [11]. The α subunit of the G_q protein activates the β isoforms of phospholipase C ($PLC\beta$), which hydrolyze the lipid phosphatidylinositol 4,5-bisphosphate (PIP2) to generate the second messengers inositol 1,4,5-trisphosphate (IP3) and diacylglycerol (DAG) [12]. The second messenger IP3 regulates the activity of the inositol trisphosphate receptors (IP_3R) on the surface of the endoplasmic reticulum (ER), allowing the rapid release of Ca^{2+} into the cytoplasm [13,14]. Simultaneously, the α subunit of the $G_{12/13}$ protein activates the small GTPase RhoA, known to promote cytoskeletal changes [15].

The signaling pathways described above are also common to a number of transduction systems mediated by G-protein coupled receptors in other cell types. We have recently published a model of PAR1 signaling in platelets ([13]).

In [4], several kinetic parameters had to be inferred because they were unknown and/or difficult to measure. In this work, we analyzed the influence of the chosen parameters to the system’s output. We performed a sensitivity test based on the Taylor expansion of the output functions around the chosen input parameters (local analysis) and a sensitivity test based on Monte Carlo sampling techniques of the system parameters (global analysis). Our results show that although the two techniques implemented are conceptually different, they lead, at least qualitatively, to consistent results. We show that the system is not sensitive to the majority of the parameters chosen in [4] and we identify three important nodes in the model. These results represent a further test for the validity of the model in [4]. Additionally, this analysis will help design more refined computational models, and will have the ultimate goal of identifying influential parameters and key signaling nodes with possible applications in biology and medicine.

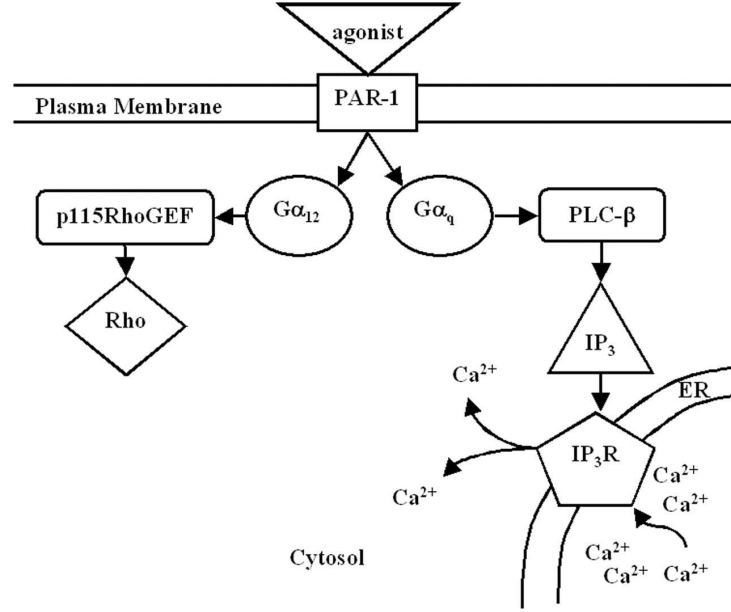


Figure 1. Pictorial representation of PAR1-mediated signaling pathways in endothelial cells. Upon cell stimulation by a PAR1 agonist peptide such as SFLLRN, PAR1 simultaneously activates the two classes of G proteins, G_q and G_{12/13}. The α subunit of the G_q protein activates the β isoforms of phospholipase C (PLCβ), which hydrolyze the lipid phosphatidylinositol 4,5-bisphosphate (PIP2) to generate the second messengers inositol 1,4,5-trisphosphate (IP3). IP3 then regulates the activity of the inositol trisphosphate receptors (IP₃R) on the surface of the endoplasmic reticulum (ER) allowing the rapid release of Ca²⁺ into the cytoplasm. Simultaneously, the α subunit of the G_{12/13} protein activates the small GTPase Rho to promote cytoskeletal changes. Reproduced from [4].

Methods

Sensitivity Analysis by Taylor Expansion

Consider a mathematical model defined by the following q -dimensional system of ordinary differential equations (ODEs) with initial conditions \mathbf{y}_o ,

$$\begin{cases} \dot{\mathbf{y}} &= f(\mathbf{y}, \mathbf{k}) \\ \mathbf{y}_o &= \mathbf{y}(0), \end{cases} \quad (1)$$

where $\mathbf{y} = (y_1, \dots, y_q)$ is the q -dimensional vector of system states and $\mathbf{k} = (k_1, \dots, k_n)$ is the n -dimensional vector of input parameters. A simple estimate of the effect of the uncertainties in \mathbf{k} on \mathbf{y} ,

Table 1. The sensitivity coefficients calculated by the Taylor-like formula at the peak time t_i for Ca^{2+} and RhoGTP

k	Ca^{2+}		RhoGTP		FUNCTIONAL ROLE
	S_+	S_-	S_+	S_-	
1	0.000	0.002	0.012	0.038	PAR1 activation by SFLLRN
2	0.000	0.000	0.000	0.000	
3	-0.001	0.001	-0.004	-0.018	
7	-0.006	-0.006	-0.193	-0.197	PAR1 deactivation
8	0.006	0.006	-0.051	-0.050	PAR1 binding Gq
9	-0.001	-0.001	0.008	0.009	
10	0.008	0.010	0.003	-0.007	Gq releasing GDP
11	0.000	0.000	0.000	0.000	
12	0.000	0.000	0.001	0.001	Gq binding GTP
13	0.000	0.000	0.000	0.000	
14	0.019	0.024	0.056	0.053	Gq releasing $\beta\gamma$
15	0.000	0.000	0.000	0.000	
16	0.000	0.000	0.000	0.000	Gq deactivation
17	0.000	0.000	0.014	0.000	PLC β binding GqGTP
18	0.000	0.000	0.000	0.000	
19	-0.040	-0.034	-0.018	-0.003	PLC β hydrolyzing GqGTP
20	0.000	0.000	0.000	0.000	PLC β releasing GqGDP
21	0.000	0.000	0.000	0.000	
22	0.032	0.042	0.007	0.013	PLC β binding PIP2
23	0.000	0.000	0.000	0.000	
24	0.000	0.000	0.000	0.000	PLC β hydrolyzing PIP2
25	-0.065	-0.066	-0.016	-0.009	Consumption of IP3
26	0.000	0.000	0.245	0.247	PAR1 binding G13
27	0.000	0.000	-0.041	-0.041	
28	0.000	0.000	0.039	0.042	G13 releasing GDP
29	0.000	0.000	0.000	0.000	
30	0.000	0.000	0.000	0.000	G13 binding GTP
31	0.000	0.000	0.000	0.000	
32	0.000	0.000	-0.001	-0.001	G13 releasing $\beta\gamma$
33	0.000	0.000	0.000	0.000	
34	0.000	0.000	-0.022	-0.022	G13 deactivation
35	0.000	0.000	0.106	0.112	GEF binding G13GTP
36	0.000	0.000	-0.107	-0.111	
37	0.000	0.000	-0.054	-0.054	GEF hydrolyzing G13GTP
38	0.000	0.000	0.000	0.000	GEF releasing G13GDP
39	0.000	0.000	0.000	0.000	
40	0.000	0.000	0.249	0.251	GEFG13GTP binding RhoGDP
41	0.000	0.000	-0.017	-0.017	
42	0.000	0.000	0.017	0.018	Rho activation
43	0.000	0.000	-0.199	-0.203	Rho deactivation

The sensitivity coefficients $S_{ij}(t, \bar{\mathbf{k}}) = \left. \frac{\partial \ln(y_i)}{\partial \ln(k_j)} \right|_{\mathbf{k}=\bar{\mathbf{k}}}$ calculated at the nominal peak time t_i for $y_i = \text{Ca}^{2+}$ and variations $\Delta \mathbf{k} = \pm 5\%$ (columns two and three) and $y_i = \text{RhoGTP}$ and variations $\Delta \mathbf{k} = \pm 5\%$ (columns four and five). Sensitivity coefficients larger than 10% are in bold font. The nominal peak time t_i is defined in (5) and the coefficients S_{ij} are defined in (3).

that is, the variation of \mathbf{y} caused by a variation $\Delta \mathbf{k}$ in \mathbf{k} is

$$\Delta \mathbf{y}(t, \mathbf{k}) = \mathbf{y}(t, \bar{\mathbf{k}} + \Delta \mathbf{k}) - \mathbf{y}(t, \bar{\mathbf{k}}),$$

where $\mathbf{y}(t, \bar{\mathbf{k}})$ is a solution of (1) at time t with parameters $\mathbf{k} = \bar{\mathbf{k}}$. Assuming $|\Delta \mathbf{k}| \ll 1$, by the Taylor's

expansion in the variables \mathbf{k} about $\bar{\mathbf{k}}$,

$$\Delta \mathbf{y}(t, \mathbf{k}) = \mathbf{D}(t, \bar{\mathbf{k}}) \Delta \mathbf{k} + \mathbf{O}(|\Delta \mathbf{k}|^2) \quad (2)$$

where $\mathbf{O}(|\Delta \mathbf{k}|^2)$ is a q -dimensional vector infinitesimal of order no less than 2 with respect $|\Delta \mathbf{k}|$, and $\mathbf{D}(t, \bar{\mathbf{k}})$ is the $n \times q$ matrix of the partial derivatives at $\bar{\mathbf{k}}$ of entries

$$\mathbf{D}(t, \bar{\mathbf{k}}) = \left(\frac{\partial y_i}{\partial k_j}(t, \mathbf{k}) \right) \Bigg|_{\mathbf{k}=\bar{\mathbf{k}}} \begin{array}{l} i = 1, \dots, q \\ j = 1, \dots, n \end{array}$$

Then one takes a dimensionless version of $\mathbf{D}(t, \bar{\mathbf{k}})$ as a measure of the sensitivity of the system at time t , with respect to the set of parameters \mathbf{k} . Precisely one introduces a *sensitivity matrix* $\mathbf{S}(t, \bar{\mathbf{k}})$ of entries

$$S_{ij}(t, \bar{\mathbf{k}}) = \frac{\partial \ln(y_i)}{\partial \ln(k_j)} \Bigg|_{\mathbf{k}=\bar{\mathbf{k}}} = \frac{\bar{k}_j}{y_i(t, \bar{\mathbf{k}})} \frac{\partial y_i(t, \mathbf{k})}{\partial k_j} \Bigg|_{\mathbf{k}=\bar{\mathbf{k}}} \quad (3)$$

and takes $S_{ij}(t, \bar{\mathbf{k}})$ as a measure of the sensitivity of the system state $y_i(t, \mathbf{k})$ at time t with respect to the kinetic parameter k_j about the nominal values $\bar{\mathbf{k}}$. In the context of the kinetic model in [4] we selected the states

$$y_i(t, \mathbf{k}) = [\text{Ca}^{2+}](t, \mathbf{k}) \quad (4)$$

$$y_i(t, \mathbf{k}) = [\text{RhoGTP}](t, \mathbf{k})$$

and computed $S_{ij}(t_i, \bar{\mathbf{k}})$ at time t_i where the nominal $[\text{Ca}^{2+}](t, \bar{\mathbf{k}})$ and $[\text{RhoGTP}](t, \bar{\mathbf{k}})$ attain their maximum values, e.g.,

$$y_i(t_i, \bar{\mathbf{k}}) = \max_t y_i(t, \bar{\mathbf{k}}). \quad (5)$$

The sensitivity coefficients $S_{ij}(t_i, \bar{\mathbf{k}})$ for Ca^{2+} are reported in Table 1 in columns two and three along those for RhoGTP in columns four and five. The partial derivatives $\partial y_i / \partial k_j$ were approximated by discrete differences with values of $\pm 5\%$ of the nominal values and indicated respectively with the symbols S_+ and S_- .

The total output of $\mathbf{y}(\cdot, \mathbf{k})$ over the average time course T of the experiment, is

$$\mathbf{z}(\mathbf{k}) = \int_0^T \mathbf{y}(t, \mathbf{k}) dt. \quad (6)$$

Table 2. The sensitivity coefficients calculated by the Taylor-like formula over the course of the entire simulation $T = 600$ s for Ca^{2+} and RhoGTP

k	Ca^{2+}		RhoGTP		FUNCTIONAL ROLE
	Σ_+	Σ_-	Σ_+	Σ_-	
1	0.000	0.000	0.008	-0.017	PAR1 activation by SFLLRN
2	0.000	0.000	0.000	0.000	
3	0.000	0.000	-0.003	-0.013	
7	0.000	0.000	-0.449	-0.443	PAR1 deactivation
8	0.000	0.000	0.021	0.040	PAR1 binding Gq
9	0.000	0.000	-0.007	-0.007	
10	0.000	0.000	-0.001	-0.012	Gq releasing GDP
11	0.000	0.000	0.000	0.000	
12	0.000	0.000	-0.001	-0.001	Gq binding GTP
13	0.000	0.000	0.000	0.000	
14	0.000	0.000	-0.006	-0.016	Gq releasing $\beta\gamma$
15	0.000	0.000	0.000	0.000	
16	0.000	0.000	0.000	0.000	Gq deactivation
17	0.000	0.000	0.011	0.000	PLC β binding GqGTP
18	0.000	0.000	0.000	0.000	
19	0.000	0.000	-0.022	0.002	PLC β hydrolyzing GqGTP
20	0.000	0.000	0.000	0.000	PLC β releasing GqGDP
21	0.000	0.000	0.000	0.000	
22	0.000	0.000	0.001	0.019	PLC β binding PIP2
23	0.000	0.000	0.000	0.000	
24	0.000	0.000	0.000	0.000	PLC β hydrolyzing PIP2
25	-0.051	-0.057	-0.009	0.031	Consumption of IP3
26	0.000	0.000	0.423	0.429	PAR1 binding G13
27	0.000	0.000	-0.070	-0.071	
28	0.000	0.000	0.068	0.074	G13 releasing GDP
29	0.000	0.000	0.000	0.000	
30	0.000	0.000	0.000	0.000	G13 binding GTP
31	0.000	0.000	0.000	0.000	
32	0.000	0.000	0.000	0.000	G13 releasing $\beta\gamma$
33	0.000	0.000	0.000	0.000	
34	0.000	0.000	-0.199	-0.202	G13 deactivation
35	0.000	0.000	0.064	0.069	GEF binding G13GTP
36	0.000	0.000	-0.066	-0.066	
37	0.000	0.000	-0.488	-0.504	GEF hydrolyzing G13GTP
38	0.000	0.000	0.000	0.000	GEF releasing G13GDP
39	0.000	0.000	0.000	0.000	
40	0.000	0.000	0.429	0.434	GEFG13GTP binding RhoGDP
41	0.000	0.000	-0.030	-0.030	
42	0.000	0.000	0.029	0.031	Rho activation
43	0.000	0.000	-0.402	-0.421	Rho deactivation

The sensitivity coefficients $\Sigma_{ij}(\bar{\mathbf{k}}) = \frac{\bar{k}_j}{z_i(\mathbf{k})} \frac{\partial z_i(\mathbf{k})}{\partial k_j} \bigg|_{\mathbf{k}=\bar{\mathbf{k}}}$ with $\mathbf{z}(\mathbf{k}) = \int_0^T \mathbf{y}(t, \mathbf{k}) dt$ for $y_i = \text{Ca}^{2+}$ and variations $\Delta \mathbf{k} = \pm 5\%$ (columns two and three) and $y_i = \text{RhoGTP}$ and variations $\Delta \mathbf{k} = \pm 5\%$ (columns four and five). Sensitivity coefficients larger than 10% are in bold font.

For the states in (4) we chose in our simulations $T = 600$ s. The vector $\mathbf{z}(\mathbf{k})$ is independent of time and it can be expanded in Taylor's series with respect to \mathbf{k} , as in (2) with $\mathbf{D}(t, \bar{\mathbf{k}})$ replaced by its time integral over $(0, T)$. The sensitivity coefficients of $\mathbf{z}(\mathbf{k})$ about the nominal values $\bar{\mathbf{k}}$ are

$$\Sigma_{ij}(\bar{\mathbf{k}}) = \frac{\bar{k}_j}{z_i(\bar{\mathbf{k}})} \frac{\partial z_i(\mathbf{k})}{\partial k_j} \bigg|_{\mathbf{k}=\bar{\mathbf{k}}} . \quad (7)$$

The sensitivity coefficients for Ca^{2+} are reported in Table 2 in columns two and three along those for RhoGTP in columns four and five. The partial derivatives $\partial y_i / \partial k_j$ were approximated by discrete differences with values of $\pm 5\%$ of the nominal values and indicated respectively with the symbols Σ_+ and Σ_- .

The nominal values of the parameters k_j used in the sensitivity analysis described above are given in Table 3.

Monte Carlo Filtering Sensitivity Analysis

The method is based on estimating the uncertainties distributions $\mathbf{p}(\mathbf{k}) = \{p_1(k_1), \dots, p_n(k_n)\}$ of the parameters $\mathbf{k} = (k_1, \dots, k_n)$, each ranging over the intervals

$$k_j \in (k_j^{\min}, k_j^{\max}), \quad j = 1, \dots, n \quad (8)$$

and cumulatively generating the probability measure

$$\mathbf{p}(\mathbf{k})d\mathbf{k} = p_1(k_1) \cdots p_n(k_n) dk_1 \cdots dk_n$$

over the space of parameters

$$\prod_{j=1}^n (k_j^{\min}, k_j^{\max}).$$

If these ranges and uncertainties distributions were known, regarding each of the $y_i(t, \mathbf{k})$ as a random variable depending on the random \mathbf{k} one computes the mean

$$\langle y_i(t) \rangle = \int \cdots \int_{k_j^{\min}}^{k_j^{\max}} y_i(t, \mathbf{k}) \mathbf{p}(\mathbf{k}) d\mathbf{k}$$

and, the variance

$$\sigma_i^2(t) = \langle y_i^2(t) \rangle - \langle y_i(t) \rangle^2,$$

where

$$\langle y_i^2(t) \rangle = \int \cdots \int_{k_j^{\min}}^{k_j^{\max}} y_i^2(t, \mathbf{k}) \mathbf{p}(\mathbf{k}) d\mathbf{k}.$$

Table 3. Symbolic reaction schemes and effective kinetic parameters used in the simulations of the PAR1-mediated activation model of endothelial cells proposed in [4].

Symbolic Reactions	k_{\rightarrow}	k_{\leftarrow}	References
<i>Reactions governing PAR1 activation</i>			
Agonist + PAR1 \rightleftharpoons PAR1*	6.00E+04 M ⁻¹ s ⁻¹ (k_1)	1.00E-03 s ⁻¹ (k_2)	[16]
Agonist \rightarrow null	2.00E-01 s ⁻¹ (k_3)		[4]
PAR1* \rightarrow null	2.00E+01 s ⁻¹ (k_7)		[4]
<i>Reactions governing Gq activation</i>			
PAR1* + G _q GDP $\cdot \beta\gamma \rightleftharpoons$ PAR1* \cdot G _q GDP $\cdot \beta\gamma$	1.00E+08 M ⁻¹ s ⁻¹ (k_8)	1.00 s ⁻¹ (k_9)	[17]
PAR1* \cdot G _q GDP $\cdot \beta\gamma \rightleftharpoons$ PAR1* \cdot G _q $\cdot \beta\gamma$ + GDP	5.00 s ⁻¹ (k_{10})	1.00E+06 M ⁻¹ s ⁻¹ (k_{11})	[17]
PAR1* \cdot G _q $\cdot \beta\gamma$ + GTP \rightleftharpoons PAR1* \cdot G _q GTP $\cdot \beta\gamma$	1.00E+06 M ⁻¹ s ⁻¹ (k_{12})	1.00E-01 s ⁻¹ (k_{13})	[17]
PAR1* \cdot G _q GTP $\cdot \beta\gamma \rightleftharpoons$ PAR1* + G _q GTP + $\beta\gamma$	2.00 s ⁻¹ (k_{14})	1.00E+07 M ⁻² s ⁻¹ (k_{15})	[17]
G _q GTP \rightarrow G _q GDP	2.00E-02 s ⁻¹ (k_{16})		[18-20]
<i>Reactions governing IP3 and DAG generation</i>			
PLC β + G _q GTP \rightleftharpoons PLC β \cdot G _q GTP	5.00E+08 M ⁻¹ s ⁻¹ (k_{17})	5.00 s ⁻¹ (k_{18})	[20, 21]
PLC β \cdot G _q GTP \rightarrow PLC β \cdot G _q GDP	1.5E+01 s ⁻¹ (k_{19})		[19, 20]
PLC β \cdot G _q GDP \rightleftharpoons PLC β + G _q GDP	1.00E+05 s ⁻¹ (k_{20})	1.00E+02 M ⁻¹ s ⁻¹ (k_{21})	[22]
PLC β \cdot G _q GTP + PIP2 \rightleftharpoons PLC β \cdot G _q GTP \cdot PIP2	1.00E+09 M ⁻¹ s ⁻¹ (k_{22})	1.00 s ⁻¹ (k_{23})	[22]
PLC β \cdot G _q GTP \cdot PIP2 \rightarrow PLC β \cdot G _q GTP + IP3/DAG	1.00E+02 s ⁻¹ (k_{24})		[22]
IP3 \rightarrow null	2.40E-02 s ⁻¹ (k_{25})		[4]
<i>Reactions governing Ca2+ mobilization</i>			
As described previously			[14]
<i>Reactions governing G12/13 activation</i>			
PAR1* + G _{12/13} GDP $\cdot \beta\gamma \rightleftharpoons$ PAR1* \cdot G _{12/13} GDP $\cdot \beta\gamma$	1.00E+08 M ⁻¹ s ⁻¹ (k_{26})	1.00 s ⁻¹ (k_{27})	[17]
PAR1* \cdot G _{12/13} GDP $\cdot \beta\gamma \rightleftharpoons$ PAR1* \cdot G _{12/13} $\cdot \beta\gamma$ + GDP	6.00 s ⁻¹ (k_{28})	1.00E+06 M ⁻¹ s ⁻¹ (k_{29})	[17]
PAR1* \cdot G _{12/13} $\cdot \beta\gamma$ + GTP \rightleftharpoons PAR1* \cdot G _{12/13} GTP $\cdot \beta\gamma$	1.00E+06 M ⁻¹ s ⁻¹ (k_{30})	1.00E-01 s ⁻¹ (k_{31})	[17]
PAR1* \cdot G _{12/13} GTP $\cdot \beta\gamma \rightleftharpoons$ PAR1* + G _{12/13} GTP + $\beta\gamma$	2.00 s ⁻¹ (k_{32})	1.00E+07 M ⁻² s ⁻¹ (k_{33})	[17]
G _{12/13} GTP \rightarrow G _{12/13} GDP	4.00E-03 s ⁻¹ (k_{34})		[23, 24]
<i>Reactions governing Rho activation</i>			
GEF _{Rho} + G _{12/13} GTP \rightleftharpoons GEF _{Rho} \cdot G _{12/13} GTP	1.00E+09 M ⁻¹ s ⁻¹ (k_{35})	3.00 s ⁻¹ (k_{36})	[20]
GEF _{Rho} \cdot G _{12/13} GTP \rightarrow GEF _{Rho} \cdot G _{12/13} GDP	1.00E-2 s ⁻¹ (k_{36})		[23]
GEF _{Rho} \cdot G _{12/13} GDP \rightleftharpoons GEF _{Rho} + G _{12/13} GDP	1.00E+06 s ⁻¹ (k_{38})	3.00 M ⁻¹ s ⁻¹ (k_{39})	[4]
GEF _{Rho} \cdot G _{12/13} GTP + RhoGDP \rightleftharpoons GEF _{Rho} \cdot G _{12/13} GTP \cdot RhoGDP	7.70E+09 M ⁻¹ s ⁻¹ (k_{40})	7.70E+02 s ⁻¹ (k_{41})	[4]
GEF _{Rho} \cdot G _{12/13} GTP \cdot RhoGDP \rightarrow GEF _{Rho} \cdot G _{12/13} GTP + RhoGTP	1.03E+04 s ⁻¹ (k_{42})		[4]
RhoGTP \rightarrow RhoGDP	6.00E-02 s ⁻¹ (k_{43})		[25]

The nominal values of the parameters adopted in the PAR1-mediated activation model of endothelial cells proposed in [4]. The kinetic constants are numbered sequentially starting from the first k_{\rightarrow} (k_1) and proceeding in reading order with the exception of reaction “PAR1* \rightarrow null” which is regulated by the constant k_7 .

The variance is a measure of the influence, and relative importance, of the input \mathbf{k} to the output $\mathbf{y}(t, \mathbf{k})$ ([10]).

In practice the process is implemented in a less quantitative way, by trading the information coming from the variances $\sigma_i(t)$ with those coming from a biologically motivated *objective functional*, g_{obj} depending on one or several $y_i(t, \mathbf{k})$ [26]. Having chosen an objective functional g_{obj} , one identifies a biologically *acceptable range* for the objective function g_{obj} . For example for a *threshold value* g^{thres} of the objective functional g_{obj} one might define [26]

$$\begin{aligned} g_{\text{obj}} \leq g^{\text{thres}} & \quad \text{as the acceptable range} \\ g_{\text{obj}} > g^{\text{thres}} & \quad \text{as the non acceptable range.} \end{aligned} \quad (9)$$

Then for each k_j one determines the probability distributions $f_1(k_j)$ and $f_2(k_j)$ of those values of k_j that output the system in the acceptable or non acceptable range respectively. For each of these, and for each k_j , calculate the cumulative frequency distributions

$$cf_\ell(k_j) = \frac{\int_{k_j^{\min}}^{k_j} f_\ell(\eta) d\eta}{\max_{[k_j^{\min}, k_j^{\max}]} f_\ell(k_j)}, \quad \ell = 1, 2 \quad (10)$$

and calculate the Kolmogorov-Smirnov coefficients $d_{1,2}(k_j)$ by the maximum distance function

$$d_{1,2}(k_j) = \sup_{k_j \in [k_j^{\min}, k_j^{\max}]} |cf_1(k_j) - cf_2(k_j)|. \quad (11)$$

These coefficients are taken as a measure of the relative importance of each parameter k_j on the model output. The larger the value of $d_{1,2}(k_j)$, the more important is k_j in producing the pre-defined system output [6–8, 26].

In the context of the kinetic model of [4] the method is implemented as follows:

1. Select nominal values $\bar{\mathbf{k}} = (\bar{k}_1, \dots, \bar{k}_n)$ as those originally adopted in the model of [4] (see Table 3). As ranges in (8) we take intervals spanning from 1/10 to 10 times these nominal values, e.g.,

$$k_j^{\max} = 10\bar{k}_j, \quad \text{and} \quad k_j^{\min} = \frac{1}{10}\bar{k}_j.$$

On a \log_{10} scale these are symmetric intervals about $\log_{10} \bar{k}_j$.

2. Generate M random n -tuples of numbers

$$\mathbf{k}_m = (k_{1,m}, \dots, k_{n,m}) \quad \text{for } m = 1, \dots, M$$

by uniformly sampling the $\ln k_j$ from their respective symmetric uncertainty ranges defined above. In the simulations we used $M = 10,000$. Different sampling distributions (e.g. gaussian, exponential) were seen not to qualitatively affect the results.

3. Solve the system (1) for each random choice of \mathbf{k}_m , and compute the functions $\mathbf{y}(t, \mathbf{k}_m)$. Solve also (1) for the nominal values $\mathbf{k} = \bar{\mathbf{k}}$ to get the functions $\mathbf{y}(t, \bar{\mathbf{k}})$. Then for each $i = 1, \dots, q$ introduce two kinds of objective output functions of the m th trial as follows:

Objective Function at Times t_i :

$$g_{\text{obj};i}(t_i; m) = [y_i(t_i, \mathbf{k}_m) - y_i(t_i, \bar{\mathbf{k}})]^2 \quad (12)$$

where $m \in \{1, \dots, M\}$ is the m th random trial described in the previous step and the times t_i are defined in (5). For the states in (4), this function measures the variations of the of $[\text{Ca}^{2+}](t_{\text{Ca}^{2+}}, \mathbf{k})$ and $[\text{RhoGTP}](t_{\text{Rho}}, \mathbf{k})$, from their nominal maximum values. (see Table 4 columns two and three respectively).

Objective Function for Total Time:

Let $\mathbf{z}(\mathbf{k})$ be the total state output as in (6) and for $i = 1, \dots, q$ set

$$G_{\text{obj};i}(m) = [z_i(\mathbf{k}_m) - z_i(\bar{\mathbf{k}})]^2 \quad (13)$$

where $m \in \{1, \dots, M\}$ is the m th random trial. For the states in (4), the function $G_{\text{obj};i}(m)$ measures the perturbation of the total outputs of Ca^{2+} and RhoGTP over the time course T of the experiment, from their nominal values. The results are compared in Table 5 in columns two and three.

Table 4. The sensitivity coefficients calculated by Monte Carlo filtering at the nominal peak time t_i for Ca^{2+} and RhoGTP

k	$d_{1,2}$		FUNCTIONAL ROLE
	Ca^{2+}	RhoGTP	
1	0.095	0.084	PAR1 activation by SFLLRN
2	0.031	0.026	
3	0.113	0.093	
7	0.160	0.285	PAR1 deactivation
8	0.091	0.153	PAR1 binding Gq
9	0.037	0.043	
10	0.072	0.017	Gq releasing GDP
11	0.017	0.022	
12	0.018	0.021	Gq binding GTP
13	0.041	0.019	
14	0.153	0.061	Gq releasing $\beta\gamma$
15	0.023	0.012	
16	0.026	0.024	Gq deactivation
17	0.024	0.033	PLC β binding GqGTP
18	0.030	0.038	
19	0.421	0.034	PLC β hydrolizing GqGTP
20	0.042	0.013	PLC β releasing GqGDP
21	0.029	0.029	
22	0.394	0.017	PLC β binding PIP2
23	0.031	0.030	
24	0.034	0.021	PLC β hydrolizing PIP2
25	0.413	0.018	Consumption of IP3
26	0.035	0.391	PAR1 binding G13
27	0.016	0.105	
28	0.027	0.068	G13 releasing GDP
29	0.018	0.026	
30	0.042	0.027	G13 binding GTP
31	0.017	0.015	
32	0.038	0.019	G13 releasing $\beta\gamma$
33	0.023	0.048	
34	0.017	0.073	G13 deactivation
35	0.021	0.158	GEF binding G13GTP
36	0.024	0.196	
37	0.026	0.170	GEF hydrolizing G13GTP
38	0.016	0.043	GEF releasing G13GDP
39	0.026	0.025	
40	0.042	0.385	GEFG13GTP binding RhoGDP
41	0.024	0.104	
42	0.029	0.031	Rho activation
43	0.023	0.350	Rho deactivation

The sensitivity coefficients measured as Kolmogorov-Smirnov distances $d_{1,2}$ estimated in the ranges $[1/10, 10]\bar{k}_j$ at the nominal peak time t_i for $y_i = \text{Ca}^{2+}$ (column two) and $y_i = \text{RhoGTP}$ (column three). Sensitivity coefficients larger than 10% are in bold font. The nominal peak time t_i is defined in (5) and the objective function used in the simulations is defined in (12).

4. Introduce threshold values

$$\begin{aligned}
 g_{\text{obj};i}^{\text{thres}}(t_i) &= \frac{1}{M} \sum_{m=1}^M g_{\text{obj};i}(t_i; m) \\
 G_{\text{obj};i}^{\text{thres}} &= \frac{1}{M} \sum_{m=1}^M G_{\text{obj};i}(m).
 \end{aligned} \tag{14}$$

The m th random trial and its parameters \mathbf{k}_m are deemed *acceptable* according to the criterion in (9) for each of these objective functions and their respective threshold values. On the basis of this classification, generate the probability distribution functions $f_1(k_j)$ and $f_2(k_j)$ of acceptable and unacceptable values,

Table 5. The sensitivity coefficients calculated by Monte Carlo filtering over the course of the entire simulation $T = 600$ s for Ca^{2+} and RhoGTP

k	$d_{1,2}$		FUNCTIONAL ROLE
	Ca^{2+}	RhoGTP	
1	0.042	0.032	PAR1 activation by SFLLRN
2	0.034	0.029	
3	0.045	0.071	
7	0.171	0.208	PAR1 deactivation
8	0.109	0.049	PAR1 binding Gq
9	0.041	0.017	
10	0.044	0.017	Gq releasing GDP
11	0.017	0.018	
12	0.046	0.021	Gq binding GTP
13	0.020	0.029	
14	0.034	0.023	Gq releasing $\beta\gamma$
15	0.030	0.019	
16	0.031	0.038	Gq deactivation
17	0.021	0.050	PLC β binding GqGTP
18	0.020	0.028	
19	0.157	0.022	PLC β hydrolizing GqGTP
20	0.035	0.030	PLC β releasing GqGDP
21	0.042	0.011	
22	0.085	0.020	PLC β binding PIP2
23	0.020	0.013	
24	0.028	0.018	PLC β hydrolizing PIP2
25	0.216	0.043	Consumption of IP3
26	0.032	0.141	PAR1 binding G13
27	0.034	0.041	
28	0.026	0.044	G13 releasing GDP
29	0.031	0.048	
30	0.033	0.028	G13 binding GTP
31	0.022	0.024	
32	0.050	0.021	G13 releasing $\beta\gamma$
33	0.029	0.017	
34	0.038	0.066	G13 deactivation
35	0.034	0.058	GEF binding G13GTP
36	0.029	0.111	
37	0.033	0.125	GEF hydrolizing G13GTP
38	0.058	0.011	GEF releasing G13GDP
39	0.033	0.016	
40	0.044	0.105	GEFG13GTP binding RhoGDP
41	0.045	0.052	
42	0.052	0.039	Rho activation
43	0.037	0.238	Rho deactivation

The sensitivity coefficients measured as Kolmogorov-Smirnov distances $d_{1,2}$ estimated in the ranges $[1/10, 10] \bar{k}_j$ over the course of the entire simulation $T = 600$ s for $y_i = \text{Ca}^{2+}$ (column two) and $y_i = \text{RhoGTP}$ (column three). Sensitivity coefficients larger than 10% are in bold font. The objective function used in the simulations is defined in (13).

relative to $g_{\text{obj};i}(t_i; m)$ and $G_{\text{obj};i}(m)$ respectively.

5. Calculate the cumulative frequency distributions $cf_\ell(k_j)$ as in (10) relative to each objective function, and the corresponding Kolmogorov-Smirnov coefficient $d_{1,2}(k_j)$ as in (11). The larger the value of $d_{1,2}(k_j)$ the higher the sensitivity of the system to the variation of the corresponding parameter.

All the calculations were performed on a MATLAB (R2009b, The Mathworks, Natick, MA) platform.

Times to Peak and Peak Values

Table 6. The sensitivity coefficients calculated by Monte Carlo filtering for the peak values of Ca^{2+} and RhoGTP

k	$d_{1,2}$		FUNCTIONAL ROLE
	Ca^{2+}	RhoGTP	
1	0.091	0.082	PAR1 activation by SFLLRN
2	0.030	0.027	
3	0.102	0.100	
7	0.218	0.280	PAR1 deactivation
8	0.160	0.120	PAR1 binding Gq
9	0.063	0.035	
10	0.073	0.014	Gq releasing GDP
11	0.026	0.012	
12	0.028	0.026	Gq binding GTP
13	0.054	0.016	
14	0.138	0.055	Gq releasing $\beta\gamma$
15	0.024	0.017	
16	0.027	0.021	Gq deactivation
17	0.020	0.036	PLC β binding GqGTP
18	0.038	0.047	
19	0.404	0.030	PLC β hydrolyzing GqGTP
20	0.029	0.016	PLC β releasing GqGDP
21	0.032	0.035	
22	0.438	0.019	PLC β binding PIP2
23	0.038	0.019	
24	0.014	0.017	PLC β hydrolyzing PIP2
25	0.386	0.022	Consumption of IP3
26	0.041	0.375	PAR1 binding G13
27	0.017	0.112	
28	0.028	0.059	G13 releasing GDP
29	0.031	0.018	
30	0.022	0.025	G13 binding GTP
31	0.019	0.021	
32	0.021	0.019	G13 releasing $\beta\gamma$
33	0.018	0.038	
34	0.038	0.077	G13 deactivation
35	0.023	0.160	GEF binding G13GTP
36	0.027	0.206	
37	0.022	0.130	GEF hydrolyzing G13GTP
38	0.036	0.038	GEF releasing G13GDP
39	0.024	0.022	
40	0.037	0.370	GEFG13GTP binding RhoGDP
41	0.021	0.096	
42	0.024	0.035	Rho activation
43	0.020	0.344	Rho deactivation

The sensitivity coefficients measured as Kolmogorov-Smirnov distances $d_{1,2}$ estimated in the ranges $[1/10, 10] \bar{k}_j$ for the peak values of $y_i = \text{Ca}^{2+}$ (column two) and $y_i = \text{RhoGTP}$ (column three). Sensitivity coefficients larger than 10% are in bold font. The objective function used in the simulations is defined in (16) and the peak values are defined in (17).

According to (5) the times t_i are those at when the nominal states $y_i(\cdot, \bar{\mathbf{k}})$ achieve their peak value. The states $y_i(\cdot, \mathbf{k})$ however achieve their peak values at times t_i^{peak} which, in general differ from t_i and are in general functions of \mathbf{k} . Set

$$y_i^{\max}(\mathbf{k}) = y_i(t_i^{\text{peak}}(\mathbf{k}), \mathbf{k}) = \max_t y_i(t, \mathbf{k}). \quad (15)$$

Table 7. The sensitivity coefficients calculated by Monte Carlo filtering for the peak times t_i^{peak} of Ca^{2+} and RhoGTP

k	$d_{1,2}$		FUNCTIONAL ROLE
	Ca^{2+}	RhoGTP	
1	0.075	0.043	PAR1 activation by SFLLRN
2	0.032	0.028	
3	0.031	0.034	
7	0.201	0.530	PAR1 deactivation
8	0.134	0.441	PAR1 binding Gq
9	0.063	0.161	
10	0.081	0.076	Gq releasing GDP
11	0.071	0.032	
12	0.074	0.032	Gq binding GTP
13	0.033	0.045	
14	0.199	0.338	Gq releasing $\beta\gamma$
15	0.067	0.045	
16	0.076	0.023	Gq deactivation
17	0.052	0.042	PLC β binding GqGTP
18	0.033	0.032	
19	0.148	0.039	PLC β hydrolizing GqGTP
20	0.025	0.040	PLC β releasing GqGDP
21	0.035	0.046	
22	0.324	0.039	PLC β binding PIP2
23	0.051	0.040	
24	0.066	0.040	PLC β hydrolizing PIP2
25	0.318	0.022	Consumption of IP3
26	0.038	0.083	PAR1 binding G13
27	0.023	0.039	
28	0.032	0.059	G13 releasing GDP
29	0.040	0.030	
30	0.027	0.046	G13 binding GTP
31	0.052	0.016	
32	0.056	0.027	G13 releasing $\beta\gamma$
33	0.047	0.065	
34	0.067	0.314	G13 deactivation
35	0.044	0.063	GEF binding G13GTP
36	0.064	0.083	
37	0.034	0.448	GEF hydrolizing G13GTP
38	0.029	0.044	GEF releasing G13GDP
39	0.030	0.042	
40	0.067	0.045	GEFG13GTP binding RhoGDP
41	0.046	0.051	
42	0.060	0.034	Rho activation
43	0.029	0.059	Rho deactivation

The sensitivity coefficients measured as Kolmogorov-Smirnov distances $d_{1,2}$ estimated in the ranges $[1/10, 10] \bar{k}_j$ for the peak times t_i^{peak} of $y_i = Ca^{2+}$ (column two) and $y_i = RhoGTP$ (column three). Sensitivity coefficients larger than 10% are in bold font. The objective function used in the simulations is defined in (16) and the peak times t_i^{peak} are defined in (15).

Dose responses for different concentrations of agonists are measured at t_i^{peak} . In practice, for a set of parameters \mathbf{k} , which in general is unknown, this is done by recording the experimental outputs $y_i^{max}(\mathbf{k})$. For small variations of \mathbf{k} about its nominal vector $\bar{\mathbf{k}}$, the sensitivity of $y_i^{max}(\mathbf{k})$ could be theoretically “measured” as in (3), by the sensitivity matrix of entries

$$S_{ij}^{peak}(\bar{\mathbf{k}}) = \frac{\partial \ln y_i^{max}}{\partial \ln(k_j)} \Big|_{\mathbf{k}=\bar{\mathbf{k}}} = \frac{\bar{k}_j}{y_i^{max}(\bar{\mathbf{k}})} \left\{ \frac{\partial y_i(t_i^{peak}(\mathbf{k}), \mathbf{k})}{\partial k_j} + \frac{dy_i(t_i^{peak}(\mathbf{k}), \mathbf{k})}{\partial t} \frac{\partial t_i^{peak}(\mathbf{k})}{\partial k_j} \right\} \Big|_{\mathbf{k}=\bar{\mathbf{k}}}$$

This formula however requires the form of the functions $\mathbf{k} \rightarrow t_i^{\text{peak}}(\mathbf{k})$, which are in general not know. Alternatively, the analysis can be carried by the filtering method, by introducing two new objective functions:

$$\begin{aligned} F_{Y_i}^{\text{peak}}(m) &= [y_i^{\text{max}}(\mathbf{k}_m) - y_i(t_i, \bar{\mathbf{k}})]^2 \\ T_{Y_i}^{\text{peak}}(m) &= [t_i^{\text{peak}}(\mathbf{k}_m) - t_i]^2 \end{aligned} \quad (16)$$

where the vector \mathbf{k}_m is the output of the m th random trial. Threshold values and distribution functions can be defined and determined as above. For $y_i = [\text{Ca}^{2+}]$ and $y_i = [\text{RhoGTP}]$, denote their peak times by $t_{\text{Ca}^{2+}}^{\text{peak}}$ and $t_{\text{Rho}}^{\text{peak}}$ respectively, and set

$$\begin{aligned} [\text{Ca}^{2+}]^{\text{max}}(\mathbf{k}) &= [\text{Ca}^{2+}](t_{\text{Ca}^{2+}}^{\text{peak}}(\mathbf{k}), \mathbf{k}) \\ [\text{RhoGTP}]^{\text{max}}(\mathbf{k}) &= [\text{RhoGTP}](t_{\text{Rho}}^{\text{peak}}(\mathbf{k}), \mathbf{k}). \end{aligned} \quad (17)$$

Then the first of (16) measures the variations of the peak values of $[\text{Ca}^{2+}]$ and $[\text{RhoGRP}]$ from their peak nominal values, whereas the second of (16) measures the variation of their times to peak $t_{\text{Ca}^{2+}}^{\text{peak}}$ and $t_{\text{Rho}}^{\text{peak}}$ respectively, from their nominal values $t_{\text{Ca}^{2+}}$ and t_{RhoGTP} . The results are reported in Tables 6 and 7 respectively.

Results and Discussion

We performed sensitivity analysis of a previously derived PAR1-mediated activation model of endothelial cells. We used two different techniques, one based on the Taylor expansion of the system's output around the nominal values of its input parameters k_j and the second based on Monte Carlo sampling techniques of the model parameters. The analysis based on the Taylor expansions (2) and leading to the sensitivity matrices $S_{ij}(t_i, \bar{\mathbf{k}})$ in (3) and $\Sigma_{ij}(\bar{\mathbf{k}})$ in (7), imposes two restrictions. The first is that $|\Delta \mathbf{k}| \ll 1$ with the notion of "smallness" depending on a predefined notion of smallness of $|\Delta \mathbf{y}|$. The second is that these matrices measure the relative variation of y_i and z_i with respect to k_j , by keeping all the remaining parameters fixed, thereby neglecting the cumulative effects of $\Delta \mathbf{k}$.

The analysis based on the Kolmogorov-Smirnov test, does not require the range of \mathbf{k} to be small, however it does require that the uncertainty distributions $\mathbf{p}(\mathbf{k})$ be known. The method leaves open the choice of the objective function. This on the one hand affords the flexibility in tailoring the objective function to specific experimental processes, and on the other hand allows non quantitative elements in

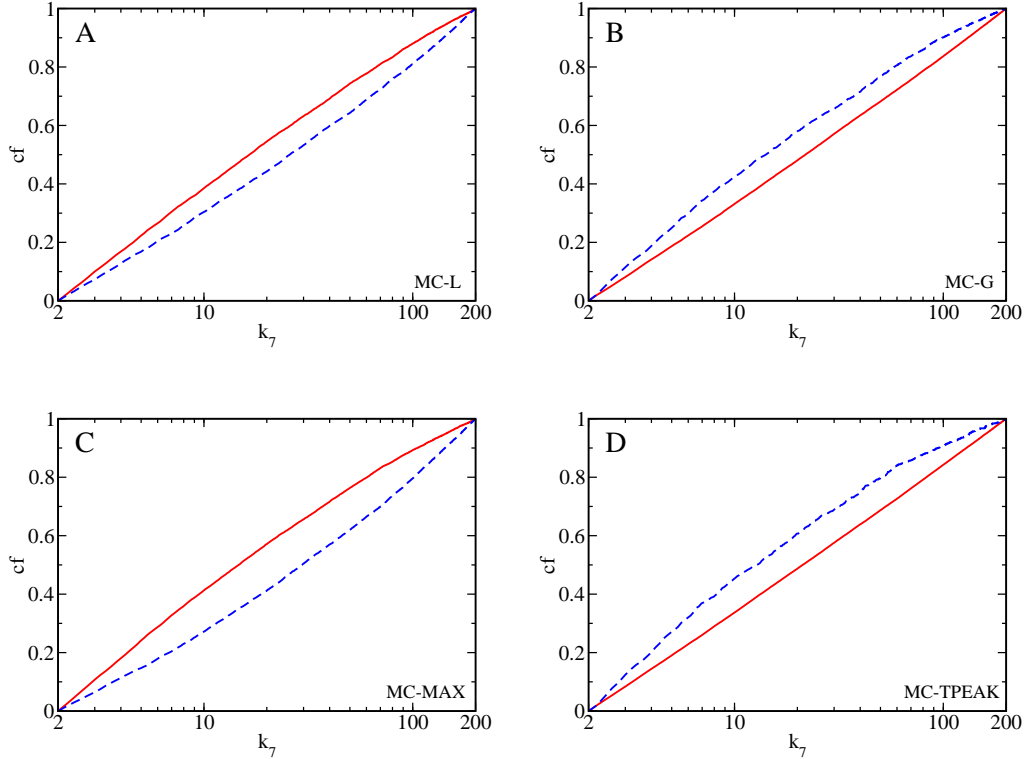


Figure 2. Cumulative distribution functions of the most influential kinetic parameter k_7 for the output $y_i = \text{Ca}^{2+}$. The red curves indicate the distributions relative to the “acceptable” sets of parameters, whereas the blue ones denote those corresponding to the “unacceptable” set of parameters (see **Methods**). Panel A: Monte Carlo filtering method results at the nominal peak time t_i . Panel B: Monte Carlo filtering results for the entire time-course of the simulation, $T = 600$ s. Panel C: Monte Carlo filtering results for the peak values $[\text{Ca}^{2+}]^{\text{max}}$ of the output function. Panel D: Monte Carlo filtering results for the peak times t_i^{peak} of the output function. The maximum distances between the acceptable and unacceptable distributions, $d_{1,2}$ are reported in Tables 4–7 respectively and are defined in (11). The nominal peak time t_i is defined in (5) and the objective functions used are respectively (12), (13), and (16) defined in **Methods**.

the analysis.

The two methods being complementary, we performed a sensitivity analysis by using both of them, on the states in (4) arising from the mathematical model of [4].

First we analyzed the sensitivity of Ca^{2+} and RhoGTP at their nominal peak values (5) to variations of the parameters \mathbf{k} . Using the Taylor expansion method, we computed the sensitivity coefficients $S_{ij}(t_i, \bar{\mathbf{k}})$ introduced in (3) and reported them in Table 1. Using the Monte Carlo filtering method, starting from the objective function $g_{\text{obj};i}(t_i; m)$ introduced in (12), we computed the Kolmogorov-Smirnov coefficients by the distance function in (11), and reported them in Table 4.

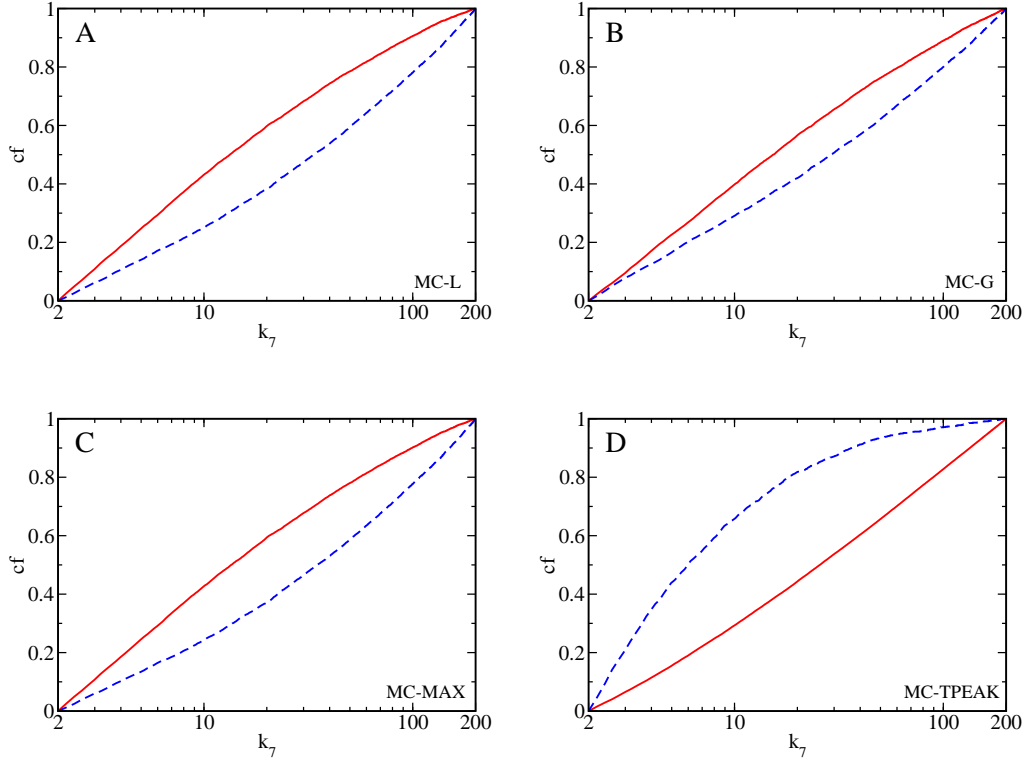


Figure 3. Cumulative distribution functions of the most influential kinetic parameter k_7 for the output $y_i = \text{RhoGTP}$. The red curves indicate the distributions relative to the “acceptable” sets of parameters, whereas the blue ones denote those corresponding to the “unacceptable” set of parameters (see **Methods**). Panel A: Monte Carlo filtering results at the nominal peak time t_i . Panel B: Monte Carlo filtering results for the entire time-course of the simulation, $T = 600$ s. Panel C: Monte Carlo filtering results for the peak values $[\text{RhoGTP}]^{\text{max}}$ of the output function. Panel D: Monte Carlo filtering results for the peak times t_i^{peak} of the output function. The maximum distances between the acceptable and unacceptable distributions, $d_{1,2}$ are reported in Tables 4–7 respectively and are defined in (11). The nominal peak time t_i is defined in (5) and the objective functions used are respectively (12), (13), and (16) defined in **Methods**.

Then we analyzed how parameters fluctuations affect the total response of Ca^{2+} and RhoGTP over the whole time course T of the experiments, quantified by the integrated states (6). We computed first the sensitivity coefficients $\Sigma_{ij}(\bar{\mathbf{k}})$ in (7), and reported in Table 2. Then, starting from the objective function $G_{\text{obj};i}(m)$ introduced in (13), we computed the Kolmogorov-Smirnov coefficients as in (11) and reported in Table 5.

Finally, by the same Monte Carlo filtering procedure we investigated the sensitivity of the peak values of Ca^{2+} and RhoGTP and their relative times to peak for cumulative variations of all the parameters k_j in intervals of 2 orders of magnitude with respect to \bar{k}_j . The results are in Table 6 and Table 7 respectively.

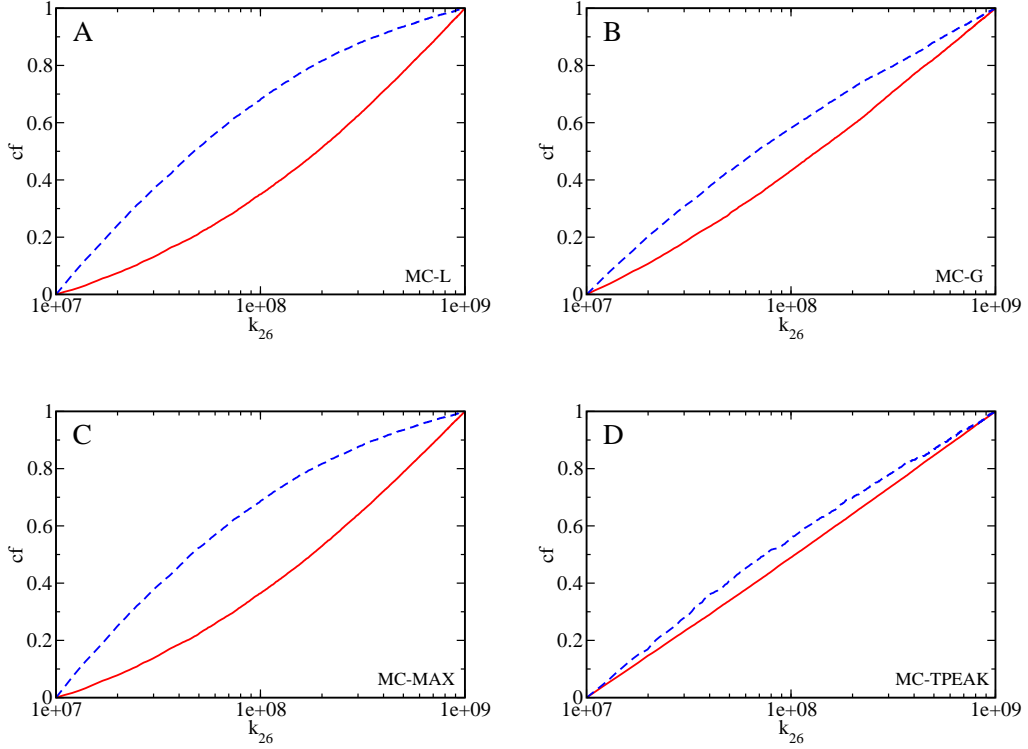


Figure 4. Cumulative distribution functions of the influential kinetic parameter k_{26} for the output $y_i = \text{RhoGTP}$. The red curves indicate the distributions relative to the “acceptable” sets of parameters, whereas the blue ones denote those corresponding to the “unacceptable” set of parameters (see **Methods**). Panel A: Monte Carlo filtering method results at the nominal peak time t_i . Panel B: Monte Carlo filtering results for the entire time-course of the simulation, $T = 600$ s. Panel C: Monte Carlo filtering results for the peak values $[\text{RhoGTP}]^{\max}$ of the output function. Panel D: Monte Carlo filtering results for the peak times t_i^{peak} of the output function. The maximum distances between the acceptable and unacceptable distributions, $d_{1,2}$ are reported in Tables 4–7 respectively and are defined in (11). The nominal peak time t_i is defined in (5) and the objective functions used are respectively (12), (13), and (16) defined in **Methods**.

As a way of analyzing and comparing the results in these tables, we deemed a parameter important for a given state $y_i(t, \mathbf{k})$ if its fluctuations about the nominal values $\bar{\mathbf{k}}$ produced sensitivity coefficients or Kolmogorov-Smirnov coefficients larger than 10%. Equivalently the state y_i was deemed not to be sensitive to variations of those parameters k_j for which the Taylor sensitivity coefficients or the Kolmogorov-Smirnov sensitivity coefficients were smaller than 10%.

The two methods are conceptually different and hence the sensitivity coefficients $S_{ij}(t_i, \bar{\mathbf{k}})$ and $\Sigma_{ij}(\bar{\mathbf{k}})$ introduced in (3) and (7) respectively, are not expected to be numerically similar to the Kolmogorov-Smirnov coefficients relative to the same processes. Nevertheless they exhibit similar qualitative results,

in the sense that most of the parameters that are important by the Taylor expansion method, are likewise important by the Monte Carlo filtering method. We first discarded those parameters to which neither Ca^{2+} and RhoGTP are sensitive by the quantitative criterion indicated above. Then in Table 8 we cross-listed those parameters to which Ca^{2+} or RhoGTP or both were sensitive. According to the adopted criterion of importance, our analysis shows that k_7 and k_8 are the most important parameters to reproduce the expected system behavior, because they respectively have ten and six entries in Table 8. In Figs. 2 and 3 ,as an example, we show the cumulative distribution functions (10) calculated by Monte Carlo filtering for the parameter k_7 in the case $y_i = \text{Ca}^{2+}$ and $y_i = \text{RhoGTP}$ respectively. The red curves represent the distribution of “acceptable” parameters, whereas the blue ones represent the distributions of “unacceptable” parameters. In panel A we report the results relative to the sensitivity test performed with the objective function calculated as in (12), panel B shows the results of the Monte Carlo filtering method with the objective function estimated according to (13), and panel C and D are relative to the choice of the objective functions in (16) respectively. Similarly, In Fig. 4, we show the cumulative distribution functions (10) calculated by Monte Carlo filtering for the parameter k_{26} in the case $y_i = \text{RhoGTP}$.

Examination of Tables 1–8 permits one to classify the input parameters into three broad categories:

RhoGTP-Only Sensitivity Parameters (four or more entries in Table 8)

- k_{26} PAR1 to G13 binding rate;
- k_{36} G13GTP-GEF dissociation rate;
- k_{37} GEF hydrolyzing G13GTP;
- k_{40} GEFG13* to Rho binding rate;
- k_{43} Rho deactivation rate.

Variations of these parameter affect only RhoGTP and its functionals

$$\begin{aligned}
 & [\text{RhoGTP}](t_i, \mathbf{k}), & \int_0^T [\text{RhoGTP}](t, \mathbf{k}) dt \\
 & [\text{RhoGTP}]^{\max}(\mathbf{k}), & t_{\text{Rho}}^{\text{peak}}(\mathbf{k})
 \end{aligned}
 \tag{18}$$

introduced in (4)–(6), and (17). Neither small variations (Taylor’s expansion), nor large variations (Monte-Carlo filtering) of these parameters about their nominal values affect Ca^{2+} and its functionals. This is an expected result as these parameters only belong to the RhoGTP module downstream of G13 (see Fig. 1).

Interestingly, our sensitivity analysis found, independently of [4], that k_{26} , which represents PAR1 binding rate to $\text{G}_{12/13}$, is a key factor in this model to reproduce the experimental data. This emerges from two different sensitivity analysis methods and constitutes a further test of validity for the signaling model adopted in [4].

Ca^{2+} -Only Sensitivity Parameters (four or more entries in Table 8)

k_{19} rate of hydrolysis of GqGTP by $\text{PLC}\beta$;

k_{22} $\text{PLC}\beta$ -PIP2 binding rate;

k_{25} IP3 rate of consumption;

Variations of these parameter affect only Ca^{2+} and its functionals

$$\begin{aligned} & [\text{Ca}^{2+}](t_i, \mathbf{k}), & \int_0^T [\text{Ca}^{2+}](t, \mathbf{k}) dt \\ & [\text{Ca}^{2+}]^{\max}(\mathbf{k}), & t_{\text{Ca}^{2+}}^{\text{peak}}(\mathbf{k}) \end{aligned} \tag{19}$$

introduced in (4)–(6), and (17). Small variations (Taylor’s expansion) or large variations (Monte-Carlo filtering) of these parameters about their nominal values do not affect RhoGTP or its functionals. Again, this is an expected result as these parameters only belong to the Ca^{2+} signaling module downstream Gq.

The presence of parameters that affect the Ca^{2+} output but not the RhoGTP output and viceversa is due to the modular structure of the model in [4]. In this model, Gq and G13 pathways are described by two separate computational modules with a common input, i.e. the activated PAR1 (Fig. 1).

The Ca^{2+} functionals in (19) are not sensitive to small variations of k_{25} (rate of IP3 consumption) about its nominal value \bar{k}_{25} (Taylor’s method for $|\Delta k_{25}| \leq 5\%$). They are however severely sensitive for variations of k_{25} in the range $(10^{-1}\bar{k}_{25}, 10\bar{k}_{25})$ (Monte Carlo filtering method).

In all cases however, the notion of “sensitivity” and “relevance” is the same by both methods, pointing to a robustness and self-consistency of the model in [4].

Table 8. List of the most important parameters as deemed by the six different sensitivity tests adopted

k	Sensitivity Analysis Method												FUNCTIONAL ROLE
	Taylor t_i		Filtering t_i		Taylor T		Filtering T		Filtering y_{max}		Filtering t_{max}		
	Ca ²⁺	RhoGTP	Ca ²⁺	RhoGTP	Ca ²⁺	RhoGTP	Ca ²⁺	RhoGTP	Ca ²⁺	RhoGTP	Ca ²⁺	RhoGTP	
3			×						×	×			Consumption PARI-AP
7		×	×	×		×	×	×	×	×	×	×	PARI deactivation
8				×			×		×	×	×	×	PARI binding Gq
9												×	
14			×						×		×	×	Gq releasing $\beta\gamma$
19			×				×		×		×		PLC β hydrolyzing GqGTP
22			×				×		×		×		PLC β binding PIP2
25			×				×		×		×		Consumption of IP3
26		×		×		×		×		×			PARI binding G13
27				×						×			
34						×						×	G13 deactivation
35		×		×						×			GEF binding G13GTP
36		×		×				×		×			
37				×		×		×		×		×	GEF hydrolyzing G13GTP
40		×		×		×		×		×			GEFG13* binding Rho
41				×									
43		×		×		×		×		×			Rho deactivation

Comparison of the sensitivity analysis results for the most important parameters reported in bold font in Tables 1–7. The symbols \times mark the importance of a given parameter k_j according to the different sensitivity test. Parameters k_7 and k_8 are important in the majority of the sensitivity tests performed.

Ca²⁺-RhoGTP Sensitivity Parameters

k_7 PAR1 deactivation rate;

k_8 PAR1-Gq binding rate;

k_{14} rate of release of $\beta\gamma$ by Gq;

PAR1 acts on the common part of the Ca²⁺ and RhoGTP pathways and accordingly both of them and their functionals are sensitive to both these parameters. While PAR1 deactivation rate k_7 is important to both Ca²⁺ and RhoGTP, the various components of the system respond differently to variations of this parameter. First, Ca²⁺ and its functionals (19), are not sensitive to small variations of k_7 about its nominal value \bar{k}_7 (Taylor's methods for $|\Delta k_7| \leq 5\%$). On the other hand all the Ca²⁺ functionals are very sensitive for variations of k_7 in the range $(10^{-1}\bar{k}_7, 10\bar{k}_7)$ (Monte Carlo filtering method).

Contrarily RhoGTP and its functionals are very sensitive to any variation k_7 , small or large, and by whatever method sensitivity is evaluated (Taylor or Monte Carlo filtering).

Finally, we observe that the pathways analyzed in this work are shared in a number of signaling cellular systems. In a recent work, we devised a mathematical model of PAR1-mediated signaling in human platelets [2] that shares several features with the model in [4]. For these reasons and for the generality of the methods adopted in this work, the conclusions of this study can, at least qualitatively, be extended to the model in [2].

References

1. Dhar PK, Zhu H, Mishra SK (2004) Computational approach to systems biology: from fraction to integration and beyond. *IEEE Trans Nanobioscience* 3: 144-52.
2. Lenoci L, Duvernay M, Satchell S, DiBenedetto E, Hamm HE (2010) Mathematical model of par1-mediated activation of human platelets. *Mol BioSyst* DOI:10.1039/C0MB00250J.
3. Purvis JE, Chatterjee MS, Brass LF, Diamond SL (2008) A molecular signaling model of platelet phosphoinositide and calcium regulation during homeostasis and P2Y1 activation. *Blood* 112: 4069-79.
4. McLaughlin JN, Shen L, Holinstat M, Brooks JD, DiBenedetto E, et al. (2005) Functional selectivity of G protein signaling by agonist peptides and thrombin for the protease-activated receptor-1. *J Biol Chem* 280: 25048-59.
5. Andreucci D, Bisegna P, Caruso G, Hamm HE, DiBenedetto E (2003) Mathematical model of the spatio-temporal dynamics of second messengers in visual transduction. *Biophys J* 85: 1358-76.
6. Zi Z, Cho KH, Sung MH, Xia X, Zheng J, et al. (2005) In silico identification of the key components and steps in IFN- γ induced JAK-STAT signaling pathway. *FEBS Letters* 579: 1101.
7. Cho KH, Shin SY, Kolch W, Wolkenhauer O (2003) Experimental design in system biology, based on parameter sensitivity analysis using a Monte Carlo method: A case study for the TNF α -mediated NF- κ b signal transduction pathway. *Simulation* 79: 726.
8. Yoon J, Deisboeck TS (2009) Investigating differential dynamics of the MAPK signaling cascade using a multi-parametric global sensitivity analysis. *Plos One* 4: 4560.
9. Shen L, Caruso G, Bisegna P, Andreucci D, Gurevich VV, et al. (2010) Dynamics of mouse rod phototransduction and its sensitivity to variation of key parameters. *IET Syst Biol* 4: 12-32.
10. Saltelli A, Chan K, Scott M (2000) *Sensitivity Analysis*. John Wiley & Sons Ltd.
11. Coughlin SR (2000) Thrombin signalling and protease-activated receptors. *Nature* 407: 258-264.
12. Rittenhouse SE (1983) Human platelets contain phospholipase C that hydrolyzes polyphosphoinositides. *Proc Natl Acad Sci USA* 80: 5417-20.

13. Michelson AD (2007) Platelets. Academic Press.
14. Young GWD, Keizer J (1992) A single-pool inositol 1,4,5-trisphosphate-receptor-based model for agonist-stimulated oscillations in Ca^{2+} concentration. *Proc Natl Acad Sci USA* 89: 9895-9.
15. Burridge K, Chrzanowska-Wodnicka M (1996) Focal adhesions, contractility, and signaling. *Annu Rev Cell Dev Biol* 12: 463-518.
16. Ahn HS, Foster C, Boykow G, Arik L, Smith-Torhan A, et al. (1997) Binding of a thrombin receptor tethered ligand analogue to human platelet thrombin receptor. *Mol Pharmacol* 51: 350-6.
17. Zhong H, Wade SM, Woolf PJ, Linderman JJ, Traynor JR, et al. (2003) A spatial focusing model for G protein signals. Regulator of G protein signaling (RGS) protein-mediated kinetic scaffolding. *J Biol Chem* 278: 7278-84.
18. Biddlecome GH, Berstein G, Ross EM (1996) Regulation of phospholipase C-beta1 by Gq and m1 muscarinic cholinergic receptor. Steady-state balance of receptor-mediated activation and GTPase-activating protein-promoted deactivation. *J Biol Chem* 271: 7999-8007.
19. Mukhopadhyay S, Ross EM (1999) Rapid GTP binding and hydrolysis by G(q) promoted by receptor and GTPase-activating proteins. *Proc Natl Acad Sci USA* 96: 9539-44.
20. Ross EM, Wilkie TM (2000) GTPase-activating proteins for heterotrimeric G proteins: regulators of G protein signaling (RGS) and RGS-like proteins. *Annu Rev Biochem* 69: 795-827.
21. Blank JL, ABrattain K, Exton JH (1992) Activation of cytosolic phosphoinositide phospholipase C by G-protein beta gamma subunits. *J Biol Chem* 267: 23069-75.
22. Lemon G, Gibson WG, Bennett MR (2003) Metabotropic receptor activation, desensitization and sequestration-I: modelling calcium and inositol 1,4,5-trisphosphate dynamics following receptor activation. *J Theor Biol* 223: 93-111.
23. Kozasa T, Jiang X, Hart MJ, Sternweis PM, Singer WD, et al. (1998) p115 RhoGEF, a GTPase activating protein for Galpha12 and Galpha13. *Science* 1998: 2109-11.
24. Singer WD, Miller RT, Sternweis PC (1994) Purification and characterization of the alpha subunit of G13. *J Biol Chem* 269: 19796-802.

25. Yamamoto K, Kondo J, Hishida T, Teranishi Y, Takai Y (1988) Purification and characterization of a GTP-binding protein with a molecular weight of 20,000 in bovine brain membranes. Identification as the rho gene product. *J Biol Chem* 263: 9926-32.
26. Hornberger GM, Spear RC (1981) An approach to the preliminary analysis of environmental systems. *Journal of Environmental Management* 12: 7-18.